ISSN (Print) 1226-1750
ISSN (Online) 2233-6656
Journal of Magnetics 22(3), 508-513 (2017) https://doi.org/10.4283/JMAG.2017.22.3.508

Development of New Materials for the Reduction of the Magnetic Resonance Imaging Metal Artifacts and the Improvement of the Image Quality

Kyung-Seok Park[1], Ham-Gyum Kim[2], and Jae-Hwan Cho[3]*

[1]*Department of Radiology, National Cancer Center, Ilsan 10408, Republic of Korea*
[2]*Department of Radiological Technology, Ansan University, Ansan 15328, Republic of Korea*

(Received 12 June 2017, Received in final form 26 June 2017, Accepted 27 June 2017)

In the present study, a pad was developed using acetic acid in an attempt to verifiably decrease the metal- artifact presence in human subjects. The subjects of this study are 20 patients who underwent neck magnetic resonance imaging (MRI) examinations between January 2016 and December 2016. The subject ages are between 30 yr and 62 yr. First, a pad was prepared using acetic acid and a solution comprising a thickening agent and glycerin (ultrasound gel). The prepared acetic-acid gel pad was attached to the periphery of the implant and subjected to MRI. The test was carried out 20 times before and after the use of the acetic-acid gel pad. The obtained signal-to-noise ratios (SNRs) were compared in the region of interest (ROI) before and after the use of the 12 pads. As a result, the SNR was increased after the pad usage. As a result, the metal artifacts were decreased after the use of the pad. The developed pad can be used in the future as a tool for the reduction of the MRI metal artifacts.

Keywords : acetic acid, pad, metal artifacts, MRI

1. Introduction

Among the various medical-imaging devices, those of magnetic resonance imaging (MRI) are among the most valuable with one of the highest contributions to the diagnostic field. This is because the potential of MRI provides functional information as well as anatomical information, and it also visualizes molecular biological information. In addition, MRI can acquire sagittal, coronal, axial, and oblique images without changing the position of the patient because of its provision of inclinations in the three directions the slice-selection gradient, the phase-encoding gradient, and the frequency-encoding gradient [1]. Alternatively, this gradient magnetic field affects the contrast and the resolution during the image formation.

The drawbacks of MRI, however, include the metal artifact that causes an image distortion due to the susceptibility difference that is caused by the magnetism susceptibility when a metal substance containing an iron component is present [2]. In clinical practice, the internal fixation for which the stainless steel (SS) metal is used has been popularized for various musculoskeletal-instability diseases. Recently, titanium (Ti) alloy has been used instead of SS for approximately six years. The main reason is the lower likelihood of the Ti alloys regarding the development of the artifacts on MRI or computer tomography (CT) compared with SS, and the post-surgery follow-up process is straightforward. Although many experimental findings have been reported [3-5], it is not possible obtain the satisfactory image information as desired using the MRI or CT images that are obtained after the fixation of the spinal column with a Ti device [5]. Various software are being developed to reduce the metal artifacts in MRI; however, the software that has been developed so far is not available for various pulse sequences and do not represent a fundamental solution for the reduction of the metal artifacts. For this study, a pad to verifiably decrease the metal-artifact presence was developed using acetic acid.

2. Object and Method

2.1. Subject

The subjects are 20 patients who underwent a neck MRI examination between January 2016 and December 2016. The ages are between 30 yr and 62 yr. The AAPM

©The Korean Magnetics Society. All rights reserved.
*Corresponding author: Tel: +82-31-400-6941
Fax: +82-31-363-7703, e-mail: 8452404@hanmail.net

© 2017 Journal of Magnetics

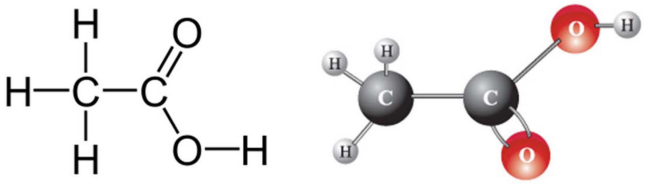

Fig. 1. (Color online) Chemical structure of acetic acid.

(American Association of Physicists in Medicine) phantom was used.

2.2. Pad production

Acetic acid and a solution comprising a thickening agent and glycerin (ultrasound gel) were mixed. The mixture ratio is 200 ml of acetic acid to 800 ml of the ultrasound gel, and a gel viscosity was achieved through the mixing process. The use of the acetic-acid formula is shown in Fig. 1. Next, the gel-form acetic acid was placed in a sanitary plastic container and stored at room temperature (15°C to 25°C). The juice shape of the acetic-acid gel pad is the same as the image shown in Fig. 2.

2.3. Experimental method

The prepared acetic-acid gel pad was attached to the periphery of the implant at the end of the test. In addition, the AAPM phantom was used for the examination (Fig. 3). The test was carried out 20 times before and after the use of the acetic-acid gel pad. MR images were acquired using a 3.0T MR scanner (ACHIVA 3.0, Philips, Netherlands) and an 8 ch NV-phased-array multi-coil. In the 3.0T MR scanner, a fat-saturation T1-weighted image (TR: time of repetition = 700 msec; TE: time of echo = 14 msec; NEX: average = 2; matrix: 512 × 512; slice thickness: 4.0 mm; FOV: field of view = 220 mm). The phantom-image acquisition was performed using a fast spin-echo (FSE) imaging method and T2-weighted image (TR = 400 msec; TE = 10 msec; NEX = 2; matrix = 512 × 512; slice thickness = 7.0 mm; FOV = 220 mm). Axial-plane images were acquired for each of the images. The acquired patient and phantom images were entered into the advantage workstation (Ver. 4.3, Revision 4. GE, USA) to measure the signal intensity. The patient's image was measured at the site of the patient before and after the use of the pad, including the neck tissue, back soft tissue, sternocleidomastoid muscle, C-spine body, longus-capitis muscle, inferior atlas facet, tongue, body axis, soft jaw tissue, and C4 vertebral body. After the image acquisition, the phantom placed the ROI at the interface, right middle outside, and left middle outside (Fig. 4). To confirm the reduction of the metal artifacts, the signal intensity was measured by as much as possible after the region of interest (ROI) drawing that includes the anatomical structure (Fig. 5). The signal-to-noise ratio (SNR) of the ROI was calculated and averaged to compare the SNRs before and after the pad usage. The SNR was calculated by dividing the signal-strength value of the ROI by the signal-intensity value of the background standard deviation. The background standard deviations of the upper-left corner and the lower-right corner were measured to achieve the SNR-effect accuracy. The equation for the SNR attainment that was applied for this experiment is as follows:

Fig. 2. (Color online) The prepared acetic-acid gel pad.

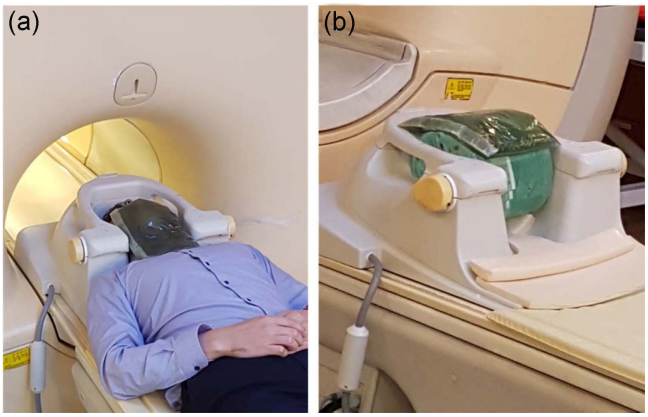

Fig. 3. (Color online) An acetic-acid gel pad was placed on the patient (a) and the phantom (b).

$$\mathrm{SNR} = \frac{\mathrm{SI\ (region,\ surrounding\ tissues)}}{\mathrm{SDN}} \quad (1)$$

SNR: signal-to-noise ratio
SDN: standard deviation of the background noise
SI: signal intensity

The difference between the mean SNR values that were

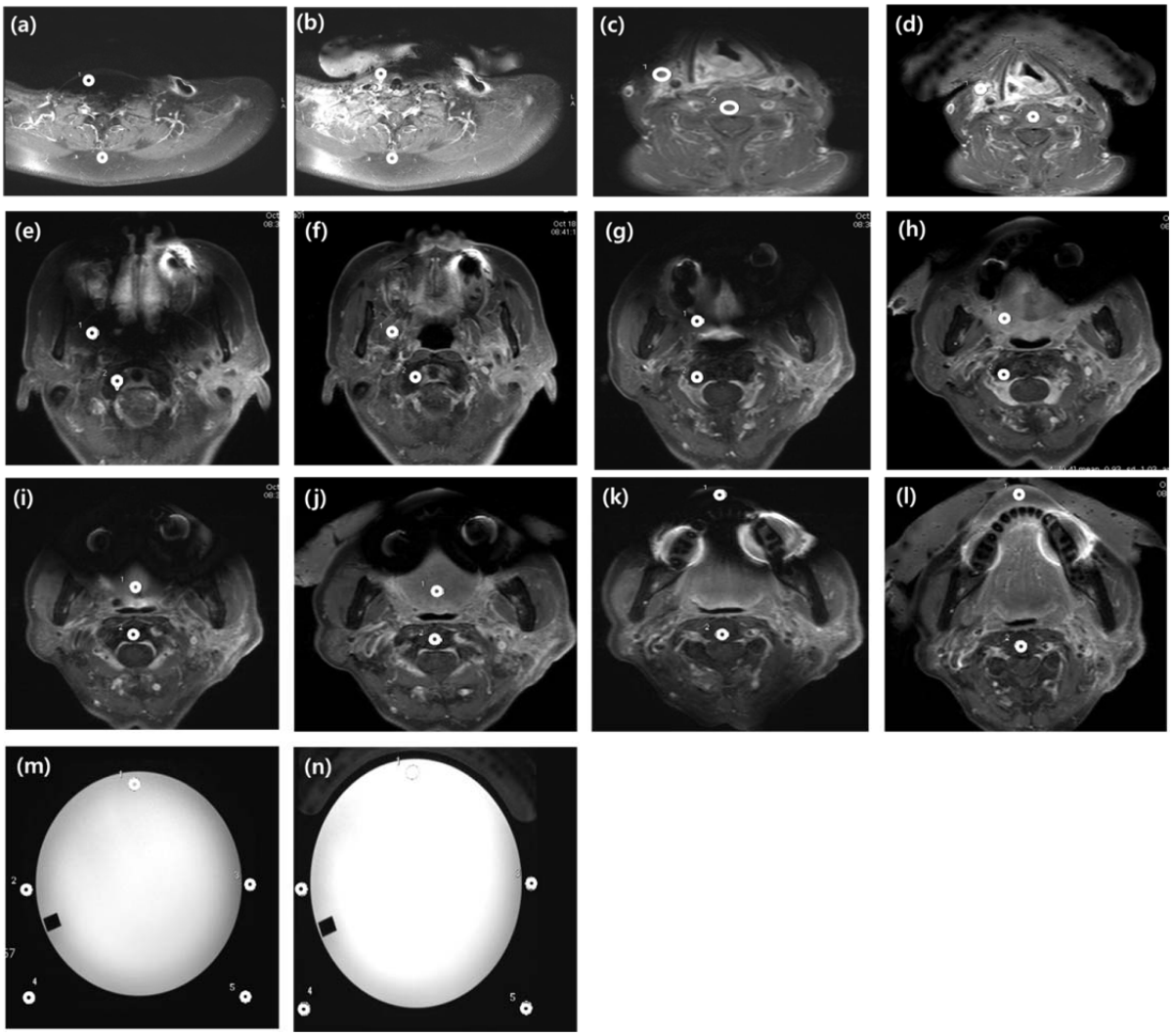

Fig. 4. The patients were divided into two groups for the following measurements: Neck tissue (a, b), back soft tissue (a, b), sternocleidomastoid muscle (c, d), C-spine body (c, d), longus-capitis muscle (e, f), inferior atlas facet (e, f), lingual tonsil (g, h), anterior atlas arch (g, h), tongue (i, j), body axis (i, j), soft tissue of jaw (k, i), and C4 vertebral body (k, i). The phantom region of interest is directly below the pad (m, n).

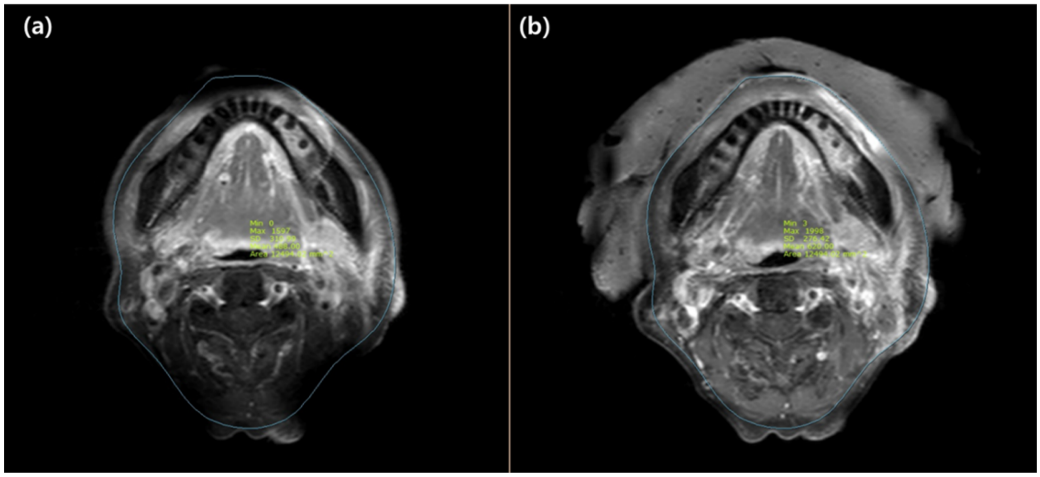

Fig. 5. (Color online) To determine whether the metal artifacts were reduced, the region of interest was drawn to include as much of the anatomical structure as possible.

Table 1. Signal-to-noise ratios values before and after the pad usage.

Measurement site	Before pad usage	After pad usage	*p*
Neck tissue	10.62 ± 3.21	48.50 ± 12.20	0.00
Back soft tissue	134.36 ± 12.35	121.79 ± 32.65	0.00
Sternocleidomastoid muscle	266.89 ± 43.25	447.58 ± 42.32	0.00
C-spine body	238.84 ± 24.65	237.95 ± 25.60	0.00
Longus capitis muscle	15.80 ± 2.10	157.25 ± 28.21	0.00
Inferior atlas facet	50.91 ± 12.35	89.02 ± 17.32	0.00
Lingual tonsil	43.08 ± 13.25	274.92 ± 25.23	0.00
Anterior atlas arch	45.68 ± 20.10	77.66 ± 10.20	0.00
Tongue	148.71 ± 16.38	176.68 ± 20.10	0.00
Body axis	44.80 ± 10.22	79.03 ± 12.21	0.00
Soft tissue of jaw	5.91 ± 1.02	150.72 ± 24.74	0.00
C4 vertebral body	58.85 ± 19.47	78.72 ± 16.23	0.00

Table 2. Signal-to-noise ratios values before and after the use of the pad in the phantom.

Measurement site	Before pad usage	After pad usage	*p*
Interface	573.78 ± 32.52	676.18 ± 27.25	0.00
Right middle outside	6.42 ± 2.23	6.34 ± 2.48	0.12
Left middle outside	4.19 ± 1.36	3.82 ± 1.68	0.14

obtained before and after the use of the pad is statistically significant throughout the corresponding T test (SPSS 18.0 for Windows). A *p*-value less than .05 represents statistical significance.

3. Results

The SNR was measured before and after the use of the pad, and the result is 10.60 ± 3.21 before the use of the pad and 48.50 ± 12.20 after the use of the pad in the neck tissue. In the sternocleidomastoid-muscle area, the pre-pad- and post-pad-use measurements are 266.89 ± 43.25 and 447.58 ± 42.32, respectively. In the longus-capitis muscle area, the pre-use and post-use measurements of 15.80 ± 2.10 and 157.25 ± 28.21, respectively, were documented. In the jaw soft tissue, the pre-use and post-use measurements of 5.91 ± 1.02 and 150.72 ± 24.74, respectively, were documented. As a result, the SNR increased after the pad usage at all of the sites ($p < 0.05$) (Table 1). As a result of the phonemic SNR analysis, the post-use SNR value at the border ROI is as large as 676.18 ± 27.25 ($p < .05$). An SNR-value difference is not evident between the right middle part and the left middle part ($p > 0.05$) (Table 2). The SNR was measured before and after the use of the pad to check whether the metal artifacts were reduced. The SNR was increased after the use of the pad ($p < .05$). As a result, the metal artifacts were decreased after the use of the pad (Table 3) (Fig. 6).

Table 3. Before and after the use of the pad to determine whether the metal artifact decreased the signal-to-noise ratios.

Before pad usage	After pad usage	*p*
128.29 ± 32.10	155.85 ± 20.10	0.00

4. Discussion

MRI has been used to obtain high-quality images in all of the directions, including the axial, coronal, and sagittal planes, and because of the bone-derived lack of bone shadow, its use frequency is increasing to determine the cause of symptoms after surgery. In the case of the patient who inserted the metal fixture, however, the artificial product was generated due to the difference of the magnetism sensitivity that is due to the gold, because the metal disrupts the surrounding magnetic field according to the magnetism, and the ROI image destruction by the artificial product is problematic [6, 7]. The susceptibility artifact indicates the degree of magnetization when a substance is exposed to a given magnetic field. Here, the relation means that a larger susceptibility difference results in a larger artifact. The artifacts that are due to the magnetic-susceptibility difference occur in the vicinity of substances with a large magnetism-sensitivity difference, and the image loss or distortion occurs at the boundary between the two substances. In addition, MRI image destruction is caused by various internal and external factors. That is, the magneto-susceptibility effect is changed by

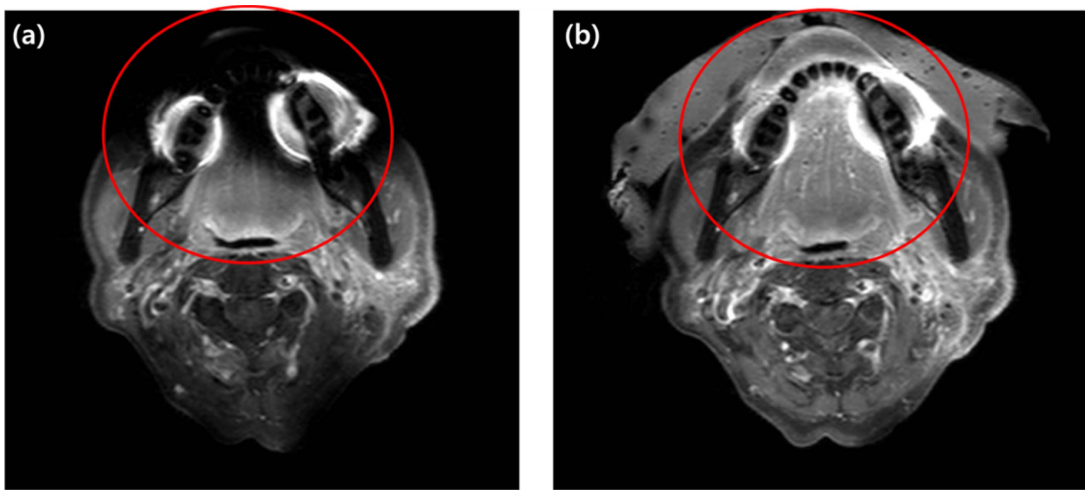

Fig. 6. (Color online) The metal artifacts were decreased after the pad usage (b) compared with the pre-use stage (a).

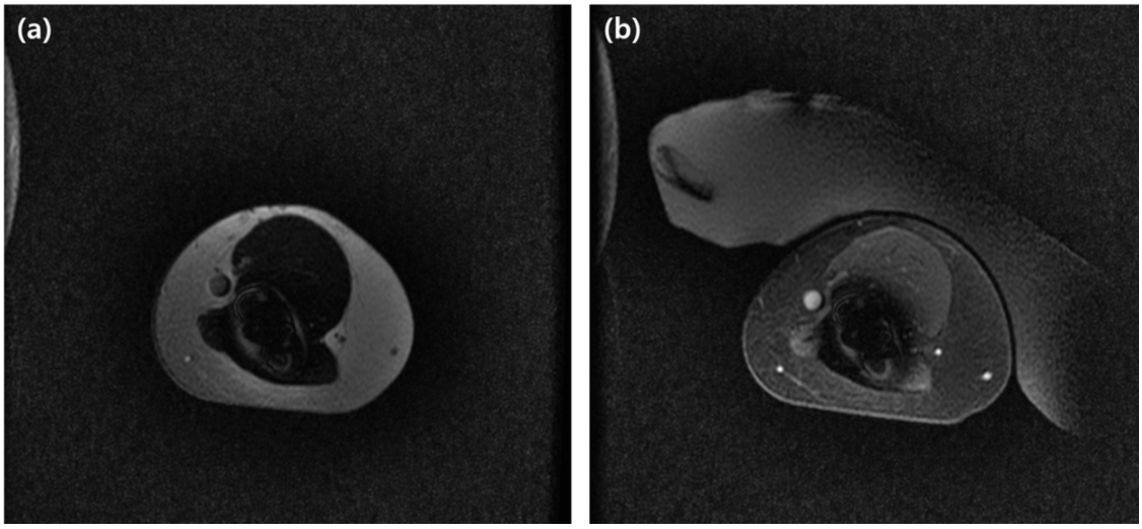

Fig. 7. The fat suppression is greater after the pad usage (b) compared with the pre-use stage (a).

factors such as the magnetic-field strength, chemical structure of the matter, and echo spacing [6]. For a given metal device, the larger the magnetic-field strength, the greater the magneto-susceptibility effect and the greater the artifact presence [4]. As a result, a major image distortion that is due to the magneto-susceptibility artifacts is observed near the region where the magneto-susceptibility difference is large like that of a metal object, and the range of the obstruction shadow is consequently widened, thereby hampering an accurate diagnosis of the lesion. Therefore, many methods have been studied to reduce the magneto-susceptibility artifacts that are caused by these metal materials. Farahan *et al.* [4] reported that the use of a fast spin-echo technique results in an echo-spacing reduction that reduces the effect of the magnetic susceptibility and reduces the MRI metal-associated artifacts; however, while the use of the fast spin-echo technique can reduce the inspection time and the magneto-susceptibility artifacts, a shaking occurs because of the different TE times of the data collection [9]. Shellock [8] reported that the increasing of the frequency bandwidth can reduce the artifacts. In addition, if the frequency bandwidth is widened, the noise is increased and the SNR of the image is decreased, thereby reducing the diagnostic efficiency of the image [10]. Efforts to reduce the metal artifacts through the development of various software have occurred [11-13]; however, the software that has been developed so far is not available for various pulse sequences and do not represent a fundamental solution for the reduction of the metal artifacts. In this study, an

acetic-acid pad was developed to reduce the metal-artifact presence. Acetic acid is less acidic than glacial acetic acid and is harmless to humans. Also, acetic acid contains a large amount of hydrogen, and an indirect energy exchange with adjacent tissues is possible. Therefore, since the susceptibility of acetic acid is high, the images can be realized through an activation of image-related tissues that are not realized due to metal substances; accordingly, the acetic-acid pad of the present study was developed. As a result of the present study, the SNR was measured before and after the use of the pad to check whether the metal artifacts had decreased. The results showed that the metal artifacts had decreased after the use of the pad. Further, metallic inserts can cause image distortions or susceptibility artifacts due to the differences in the magnetic susceptibility in relation to the surrounding tissues, rendering them incapable of reflecting sufficient imaging information [14, 15]. Also, they cause a field inhomogeneity, leading to an uneven fat suppression regarding the fat-removal techniques [16]. In this study, other parts were examined to confirm the degree of the fat suppression. As a result of the test, it was possible to confirm the achievement of a favorable fat-clearing performance for those patients with metal when the pad was used. In conclusion, the use of the developed acetic-acid pad will reduce the metal-artifact presence, as well as improving the fat erosion, thereby improving the value of the clinical diagnosis.

5. Conclusion

A variety of software have been developed to reduce the MRI metal artifacts, but the availability for various pulse sequences is lacking, and a fundamental solution for the reduction of the metal artifacts has not been achieved. For the pad that was developed for this study, the acetic acid that is used results in the reduction of the MRI metal artifacts; therefore, the developed pad can be used in the future as a tool for the reduction of the MRI metal artifacts.

References

[1] K. A. Shunk, J. A. C. Lima, A. W. Heldman, and E. Atalar, Magn. Reson. Med. **40**, 722 (1999).
[2] B. A. Hargreaves, P. W. Worters, K. B. Pauly, J. M. Pauly, K. M. Koch, and G. E. Gold, AJR Am. J. Roentgenol. **197**, 547 (2011).
[3] L. F. Czervionke, D. L. Daniels, F. W. Wehrli, L. P. Mark, L. E. Hendrix, J. A. Strandt, A. L. Williams, and V. M. Haughton, AJNR Am. J. Neuroradiol. **9**, 1149 (1988).
[4] K. Farahani, U. Sinha, S. Sinha, L. C. Chiu, and R. B. Lufkin, Comput. Med. Imaging Graph. **14**, 409 (1990).
[5] P. Stradiotti, A. Curti, G. Castellazzi, and A. Zerbi, Eur. Spine J. **18**, 102 (2009).
[6] P. L. Davis, L. E. Crooks, M. Arakawa, R. McRee, L. Kaufman, and R. M. Alexander, AJR Am. J. Roentgenol. **137**, 857 (1981).
[7] P. F. J. New, B. R. Rosen, R. J. Brady, F. S. Buonanno, J. P. Kistler, C. T. Burt, W. S. Hinshaw, J. H. Newhouse, G. M. Pohost, and J. M. Taveras, Radiology **147**, 139 (1983).
[8] F. G. Shellock, AJR Am. J. Roentgenol. **151**, 811 (1998).
[9] I. H. Huang, K. H. Emery, T. Laor, M. Valentine, and J. Tiefermann, Pediatr. Radiol. **38**, 675 (1997).
[10] C. B. Ahn, Korean Soc. Magn. Reson. Med. **8**, 42 (2004).
[11] T. K. Fehring, K. Fehring, and S. M. Odum, Clin. Orthop. Relat. Res. **473**, 574 (2015).
[12] J. M. Jennings, J. R. Martin, R. H. Kim, C. C. Yang, T. M. Miner, and D. A. Denni, J. Bone Joint Surg. Am. **99**, 593 (2017).
[13] D. H. Nawabi, S. Gold, S. Lyman, K. Fields, D. E. Padgett, and H. G. Potter, Clin. Orthop. Relat. Res. **472**, 471 (2014).
[14] O. Beuf, A. Bnguet, M. Lissac, and R. Davis, J. Magn. Reson. B **112**, 111 (1996).
[15] I. F. Schenck, Med. Phys. **23**, 815 (1996).
[16] D. G. Mitchell and M. S. Cohen, Transverse magnetization and T2 contrast. In: Mitchell, D. G., Cohen, M. S., eds. MRI principles. 2nd ed. New York, NY: Springer-Verlag (2000) pp. 35-47.